Parallel and Cross Cycloaddition of Triplet Penta-1,4-diene. An *ab initio* MO Study

Masaru Ohsaku
Department of Chemistry, Faculty of Science, Hiroshima University, Higashisenda 1-1-89, Hiroshima 730, Japan
Keiji Morokuma *
Institute for Molecular Science, Myodaiji, Okazaki 444, Japan

ab initio UHF molecular orbital calculations using the 3-21G through 6-31G* basis sets, and including spin projection and electron correlation (APUMP2), have been carried out to investigate the photosensitized cycloaddition reactions of penta-1,4-diene. Two forms of triplet penta-1,4-diene, *cis–trans*† and envelope, with nearly equal energy but with excitation localized on different bonds, are the starting points for the transition states TS1 of cross closure and TS2 of parallel closure, respectively. TS2 has a barrier of 14 kcal mol^{-1},‡ about 22 kcal mol^{-1} lower than TS1, supporting the experimental dominance of parallel closure. The transition states have structures where a significant ring strain has already developed, and the TS1 – TS2 energy difference is mainly dictated by the strain energy difference of the cyclic triplet product intermediates.

Non-conjugated aliphatic dienes are known to give bicyclic alkanes through a triplet excited state upon sensitization by the mercury ($^3P_1$) atom.[1–3] This reaction converts the dienes into 1,2-bridged cycloalkanes *via* parallel addition or into 1,3-bridged cycloalkanes *via* cross addition. The ratio of the parallel to the cross products depends on several factors. In the case of penta-1,4-diene the experimental cross:parallel ratio was found to be *ca.* 0.1,[2] the parallel closure being predominant in this species. One of the most important factors which controls the reaction is considered to be the number of methylene groups existing between the double bonds. As an explanation of these experimental results, the 'rule of five'[2] and the effect of the 'through-space' and 'through-bond interaction'[4,5] have been proposed, and are applicable to a variety of dienes.[6–8]

The only previous studies on this subject involved consideration of the photochemical reaction of penta-1,4-diene in a qualitative manner, *i.e.* using an MO method and many assumptions in geometry optimization.[9] In this paper we present the results of an *ab initio* MO study of the triplet transition states of cycloaddition of penta-1,4-diene.

Experimental

All the MO calculations were performed by using the GAUSSIAN 82 program packages,[10] and the full geometry optimization was carried out by the energy gradient procedure[11] without any symmetry restriction. The basis sets used for the calculations were the 3-21G[12] and the 6-31G*.[13] The 6-31G* UHF calculations were performed at the 3-21G UHF optimized geometries. The electron correlation was taken into account using the second order Møller–Plessett (MP2) procedure.[14] For reliable energetics elimination of spin contamination is known to be necessary. We use Yamaguchi's approximate spin projection method for both UHF and UMP2. The method will be discussed in the next section.

Results and Discussion

Optimized Geometry.—Since the cycloaddition reaction takes place only under photosensitization conditions, it is natural to assume that the reaction proceeds *via* the first triplet state. The optimized equilibrium geometries at the UHF level of penta-1,4-diene in the first triplet state are shown in Figures 1 and 2 (torsion angles are given in Table 1). There are three possible conformers with respect to the C(2)–C(3) and C(3)–C(4) axes, but only two of these *i.e.* the *cis–trans* form (**1**) and the envelope form (**3**) are shown, since the other conformer, the *trans–trans*, is not a starting point for cycloaddition. It is interesting to note that in (**1**) the excitation is localized upon the C(1)–C(2) bond, which becomes perpendicularly twisted, whereas the other double bond C(4)–C(5) remains planar. In (**3**) on the other hand, only the C(4)–C(5) double bond is excited and twisted while the C(1)–C(2) bond remains planar. Geometry optimization starting from a *cis–trans* form with the twisted C(4)–C(5) bond resulted in the optimized structure (**3**), and optimization from an envelope form with the twisted C(1)–C(2) bond gave (**1**); these starting structures therefore do not correspond to triplet equilibrium geometries. The closest distance between the two double bonds in (**1**) is 2.551 Å [*i.e.* between the C(2) and C(4) atoms], and this is too large for there to be any significant interaction between the two segments. (This will also be substantiated in a following section from the analysis of bond population). The distance between the C(2) and C(4) atoms in (**3**) is 2.509 Å; again too long for significant interaction.

We have located two transition states, TS1 and TS2, on the first triplet state, as shown in Figures 1 and 2. As will be discussed in a following section, the spin population analysis suggests that TS1, which is obviously the transition state for the cross closure, is reached from the equilibrium structure (**1**). Similarly TS2, the transition state for parallel closure, can be formed from (**3**). The C(1)–C(2) bond distance 1.392 Å in TS2 is closer to that of (**3**) (*i.e.* 1.318 Å) than the corresponding bond length of the triplet reaction product (**4**) (*i.e.* 1.516 Å), whereas the nascent C(1)–C(5) bond (2.249 Å) is closer to the corresponding value of 1.566 Å of (**4**) than that (3.790 Å) of (**3**). This suggests that the reaction is asynchronous, though concerted, in the sense that the skeletal angular changes and new bond formation occur to a greater extent before the transition state, and the C–C bond reorganization takes place mainly after the transition state. On the other hand, the C–C bond distances in TS1 resemble more closely the product (**2**) than the reactant (**1**).

† *cis–trans* refers to the conformation around C(2)–C(3) and C(3)–C(4) axes as s-*cis* and s-*trans*, or otherwise.
‡ 1 kcal = 4.184 J.

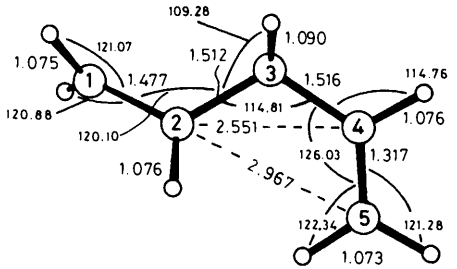

(1)

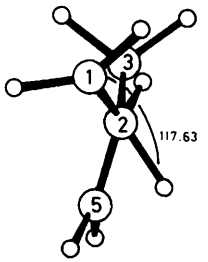

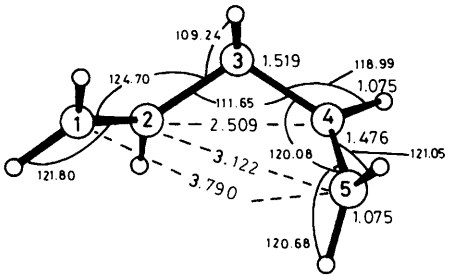

(3)

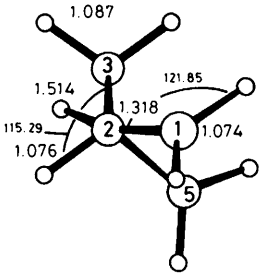

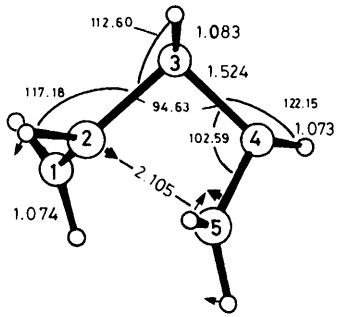

TS1

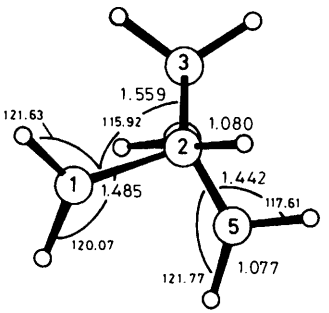

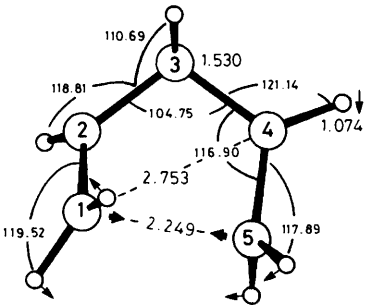

TS2

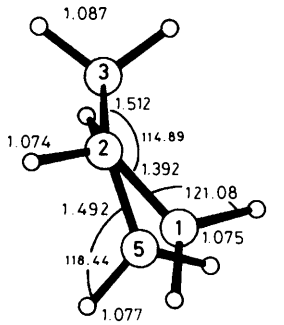

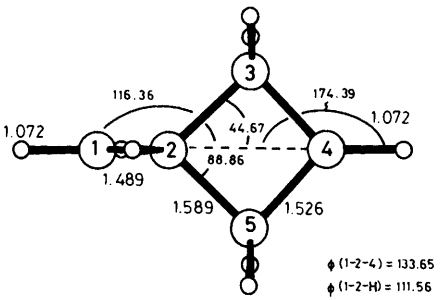

(2)

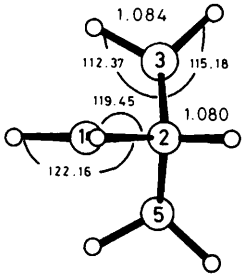

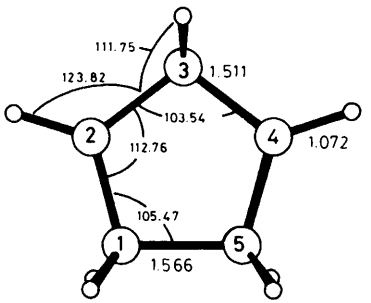

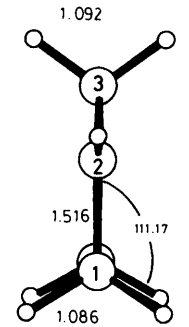

(4)

Figure 1.

Figure 2.

Figures 1 and 2. Optimized triplet structures (Å and degrees) of the reactants (**1**) and (**3**), products (**2**) and (**4**), and transition states, TS1 and TS2, at the UHF/3-21G level. Arrows are the reaction co-ordinate vector at the transition states.

Table 1. Values of torsion angles for reactants, products, and transition states.

Torsion angle/°	Compounds					
	(1)	TS1	(2)	(3)	TS2	(4)
H–C(1)–C(2)–C(3)	100.12, −78.12	103.78, −75.13	−51.37	0.25, −179.83	41.36, −161.64	120.28, −120.28
C(1)–C(2)–C(3)–C(4)	−160.36	−88.47	—	117.96	50.25	0.00
C(1)–C(2)–C(3)–H	77.61, −37.83	154.53, 30.57	−114.86, −11.33	−3.83, −121.15	97.63, −143.20	120.40, −120.40
H–C(2)–C(3)–C(4)	39.94	127.66	—	−61.54	−103.06	180.00
C(2)–C(3)–C(4)–C(5)	18.53	−29.11	—	−59.88	−21.68	0.00
C(2)–C(3)–C(4)–H	−162.77	113.31	—	134.32	165.24	180.00
C(3)–C(4)–C(5)–H	179.11, −0.59	146.27, −62.60	—	93.39, −79.77	107.82, −106.53	120.28, −120.28
H–C(1)–C(2)–C(5)	—	—	51.37	—	—	—
C(1)–C(2)–C(4)–H	—	—	0.00	—	—	—
H–C(1)–C(2)–C(4)	—	—	0.00, 180.00	—	—	—
C(1)–C(2)–C(5)–H	—	—	114.86, 11.33	—	—	—
H–C(2)–C(4)–H	—	—	180.00	—	—	—

Table 2. Atomic spin populations on the C-atoms at the UHF/3-21G level.

Structure	C(1)	C(2)	C(3)	C(4)	C(5)
(1)	1.30	1.36	−0.11	0.24	−0.18
TS1	1.37	1.16	−0.18	1.50	−1.07
(2)	1.45	−0.21	−0.06	1.57	−0.06
(3)	−0.23	0.31	−0.10	1.38	1.30
TS2	−0.96	1.26	−0.29	1.50	1.11
(4)	−0.18	1.57	−0.39	1.57	−0.18

This suggests that TS1 is later than TS2. The origin of this difference will be discussed in a subsequent section in connection with the energetics.

TS1 was confirmed to have only one imaginary vibrational frequency of 719i cm^{-1} in the normal co-ordinate analysis based on the analytical second derivatives. As shown in Figure 1, the major contribution to this normal mode arises from oscillation of the developing bond between the C(2) and C(5) atoms. Additional contributions come from the methylene deformation vibration at the C(5) atom and the C–H deformation at the C(2) atom. TS2 also has one imaginary vibrational frequency of 504i cm^{-1}. This vibration consists of the motion of the bond developing between the C(1) and C(5) atoms (Figure 2), supplemented with the C(1) and C(5) methylene deformation vibrations and the C–H deformation at the C(4) atom. TS2 has a much lower frequency than TS1, indicating that the skeleton in the earlier TS2 is softer than in the later TS1. This difference is related to the difference in the strain between four- and five-membered rings, as will be discussed.

Electron and Spin Densities.—In order to examine the characteristics of these triplet diradical species, gross atomic spin populations on the C-atoms were calculated, and these are summarized in Table 2. As will be discussed in the next section, these UHF functions are contaminated somewhat by higher spin components. The present analysis without spin projection, however, is still considered useful for qualitative discussion of the electronic structures of these species.

In (1) the spin is localized mainly on C(1) and C(2). On going from (1) to TS1 a spin polarization develops on the C(4)–C(5) bond, with a negative spin on C(5). TS1 has four unpaired electrons, which indicates substantial mixing of the quintet with the triplet. On going from TS1 to (2), a new bond is formed between antiparallel spins on C(2) and C(5). The situation is similar for TS2. On going from (3) to TS2, spin polarization develops on the C(1)–C(2) bond and in going from TS2 to (4) a new bond is formed between the antiparallel spins of C(1) and C(5).

Table 3. Net atomic and bond electron populations at the UHF/3-21G level.

		C(1)	C(2)	C(3)	C(4)	C(5)
(1)	C(1)	5.47				
	C(2)	0.29	5.55			
	C(3)	−0.08	0.26	5.46		
	C(4)	0.00	−0.07	0.26	5.26	
	C(5)	0.00	0.00	−0.08	0.54	5.21
TS1	C(1)	5.49				
	C(2)	0.25	5.71			
	C(3)	−0.09	0.25	5.52		
	C(4)	0.01	−0.21	0.27	5.59	
	C(5)	−0.01	0.08	−0.18	0.32	5.47
(2)	C(1)	5.47				
	C(2)	0.25	5.70			
	C(3)	−0.07	0.23	5.50		
	C(4)	0.01	−0.22	0.26	5.69	
	C(5)	−0.07	0.23	−0.25	0.26	5.50
(3)	C(1)	5.20				
	C(2)	0.54	5.29			
	C(3)	−0.08	0.27	5.46		
	C(4)	0.00	−0.10	0.25	5.58	
	C(5)	0.00	0.00	−0.08	0.28	5.47
TS2	C(1)	5.40				
	C(2)	0.38	5.47			
	C(3)	−0.12	0.29	5.47		
	C(4)	−0.02	−0.12	0.25	5.60	
	C(5)	0.03	−0.05	−0.09	0.29	5.51
(4)	C(1)	5.45				
	C(2)	0.26	5.61			
	C(3)	−0.09	0.27	5.44		
	C(4)	−0.08	−0.10	0.27	5.61	
	C(5)	0.25	−0.08	−0.09	0.26	5.45

Net atomic and bond electron populations on the C-atoms and the C–C bonds, respectively, are summarized in Table 3. The C(2)···C(5) bond population in (1) is zero, indicating that there is no chemical bond. In TS1 a strong bonding interaction takes place between C(2) and C(5). However, the C(2)···C(4) and C(1)···C(5) bond populations are negative, indicating a repulsive interaction. Similarly in (3) there is no interaction between C(1) and C(5) nor between C(2) and C(5). In TS2 the positive bond population between C(1) and C(5) indicates that the bond is forming between them. All other non-neighbouring bond populations remain negative, denying the possibility of bond formation between them. It is also interesting that the

bond population between C(1) and C(5) in TS2 is smaller than that between C(2) and C(5) in TS1, reflecting the earliness of TS2 in comparison with TS1.

Elimination of Spin Contamination.—It is well known that there are some spin contaminations in the results of UHF calculations.[15,16] The elimination of the spin contaminants from the UMP energies have already been discussed successfully.[17,18] The UHF/3-21G transition states obtained in the preceding section have fairly large expectation values $\langle S^2 \rangle$, *e.g.*, for TS1: 2.3898 at the UHF/3-21G level and 2.4013 at the UMP2/6-31G* level; and for TS2: 2.3368 at the UHF/3-21G level and 2.3391 at the UMP2/6-31G* level. The spin projection would be needed for a reliable estimate of an activation energy.

The 'quintet' state UHF/3-21G wave functions at TS1 and TS2 have the $\langle S^2 \rangle$ values of 6.0276 and 6.0325, respectively. Therefore one can consider that the UHF quintet state is nearly pure quintet, and only eliminate the quintet from the triplet UHF or UMP2 wave function, without worrying about higher multiplets. The energy of the approximately projected (AP) UHF or UMP2 triplet state will be estimated by the scheme by Yamaguchi *et al.*,[19] which has been applied to the analysis of thermal degenerate rearrangement in methylenecyclobutane.[20]

According to the scheme, the ^{3}UHF wave function is expressed as a sum of the projected UHF wave function (^{3}APUHF) and the quintet UHF wave function, calculated at the same geometry. The coefficient a is determined from the

$$\Psi(^3\text{UHF}) = \sqrt{1 - a^2}\Psi(^3\text{APUHF}) + a\Psi(^5\text{UHF}) \quad (1)$$

triplet UHF spin eignvalue $\langle S^2(^3\text{UHF}) \rangle$, to satisfy equation (2), where $\langle S^2(^3\text{APUHF}) \rangle = 2$ and $\langle S^2(^5\text{UHF}) \rangle = 6$ are assumed.

$$\langle S^2(^3\text{UHF}) \rangle = 2(1 - a^2) + 6a^2 \quad (2)$$

The energy of the projected triplet state is therefore given by equation (3).

$$E(^3\text{APUHF}) = [E(^3\text{UHF}) - a^2E(^5\text{UHF})]/(1 - a^2) \quad (3)$$

The weights of quintet (a^2) of the UHF/3-21G and 6-31G* wave functions for each UHF/3-21G stationary state geometry are summarized in Table 4. Equation (3) applies also to the MP2 calculation, if UHF is replaced by MP2. Since the coefficient a at the MP2 level is not easily calculable, and is not sensitive to the electron correlation, we use a value for a determined by the UHF method. As is shown in the next section, the energy lowering of TS1 and TS2 by this correction is in the range of 7.3–9.3 kcal mol^{-1}, and the lowering for reactants and products is less than 2.5 kcal mol^{-1}.

Table 4. Weights of quintet (a^2) in the triplet UHF wavefunction obtained at different levels of calculation.

	UHF/3-21G	UHF/6-31G*
(1)	0.0066	0.0051
TS1	0.0975	0.1003
(2)	0.0073	0.0070
(3)	0.0084	0.0056
TS2	0.0842	0.0848
(4)	0.0087	0.0079

Relative Energies.—The relative energies of (1), (2), (3), (4), TS1, and TS2 at the various levels of calculation are shown in Table 5. Species (1) and (3) are two rotational isomers of penta-1,4-diene in the first excited triplet state. There should be a substantial energy barrier between the two (not calculated at this time), as isomerization involves the reorganization of skeleton and dihedral angles associated with the excitation transfer. The energy difference between the two, (1) − (3), is small at all levels of calculation, and was found to be 0.6 kcal mol^{-1} at the optimum APMP2/6-31G* level. This result indicates that either of these species can be a starting point for the cycloaddition reaction.

The energy difference between TS1 and TS2 is large at all levels of calculation, with 22 kcal mol^{-1} at the APUMP2/6-31G* level, and TS2 is more favoured than TS1. As discussed above, the two initial states, (1) and (3), are nearly the same in energy, and the small difference is simply that of the activation energy. The parallel-closure *via* TS2 should therefore be much easier than the cross-closure *via* TS1 in 1,4-pentadiene. One should note, however, that the barrier for transfer from (3) to TS2 is still substantial; 14 kcal mol^{-1} at the APMP2/6-31G* (without zero-point correction). After TS1 and TS2 the energy of the system drops sharply, by 36 and 40 kcal mol^{-1}, respectively, at the APMP2/6-31G* level (without zero-point correction).

The energy difference between the two products, (2) − (4), could be related to the strain energy difference. The strain energy of cycloalkanes, commonly quoted in the literature,[21] *e.g.* cyclobutane, 26.4 kcal mol,$^{-1}$ and cyclopentane, 6.5 kcal mol,$^{-1}$ gives a difference of about 20 kcal mol.$^{-1}$ The present (2) − (4) difference of 27 kcal mol^{-1} at our best APUMP2/6-31G* level is somewhat larger than this. The present products are not precisely cycloalkanes; (2) is 3-methylcyclobutane-1,α-diyl and (4) is cyclopentane-1,3-diyl radicals in their respective triplet state. An sp^2 carbon atom in the cyclobutane ring may cause a larger additional strain energy than the sp^2 carbon atoms in the cyclopentane ring. It is also possible that the present approximation simply overestimates the difference. The energy difference between the two transition states, TS1 − TS2 = 22 kcal mol^{-1} at the APUMP2/6-31G*, is about 80% of the product energy difference discussed above, and seems to be the reflection of the latter. The geometries of TS1 and TS2 in Figures 1 and 2 indicate that a very significant skeleton deformation and hence strain has already developed. Therefore, it is reasonable to suggest that a large fraction of the product energy difference arises from the transition-state energy difference. The present results give a theoretical support to the empirical 'rule

Table 5. Relative energies (in kcal mol^{-1}) of reactants, transition states, and products at different levels of calculation at the UHF/3-21G optimized geometries.

	UHF/3-21G	APUHF/3-21G	UHF/6-31G*	APUHF/6-31G*	UMP2/6-31G*	APUMP2/6-31G*
(1)[a]	−192.800 76	−192.801 66	−193.877 92	−193.878 60	−194.468 20	−194.469 11
TS1	35.8	29.0	37.6	30.6	44.1	35.6
(2)	4.7	3.3	4.3	3.0	0.5	−0.6
(3)	−0.8	−0.9	−0.5	−0.5	−0.5	−0.6
TS2	13.0	5.8	16.9	9.7	22.5	13.7
(4)	−22.8	−24.6	−21.6	−23.3	−24.5	−26.2

[a] Total energy in hartree and the zero of relative energy.

of five.' Overall the reaction (1) ⟶ (2) is nearly thermoneutral, while the reaction (3) ⟶ (4) is exothermic by 22–26 kcal mol^{-1} at various levels of calculation. The indication of the calculated transition-state geometries in Figures 1 and 2, *i.e.* that TS2 is earlier than TS1, can also be considered to reflect this thermochemical difference.

Conclusions

The present theoretical study has led to the following conclusions: (*a*) the energy difference between the *cis–trans* and the envelope forms of the reactant, penta-1,4-diene, in the triplet state is very small, and both forms are probably produced in the initial stage of reaction. The geometries of the two forms are quite different, with the excitation localized on the external C=C bond in the former and on the internal C=C bond in the latter; (*b*) the transition state for parallel closure, which can be reached only from the envelope form, has a substantially lower energy than that for cross closure, the latter being attainable only from the *cis–trans* form; (*c*) the analysis of the transition-state structures indicates that the energy difference between the two transition states is mainly determined by the strain energy and is parallel to that expected in the product.

These conclusions are consistent with experimental results, but can only be obtained from a theoretical study that can model the 'inside' of the reaction potential energy surfaces, which are 'invisible' to less rigorous mathematical investigations.

Acknowledgements

All the computations were carried out at the IMS Computer Center. This work was supported by the Joint Studies Program (1988–1989) of the Institute for Molecular Science.

References

1 R. J. Cvetanovic, H. E. Gunning, and E. W. R. Steacie, *J. Chem. Phys.*, 1959, **31**, 573.
2 R. Srinivasan, *J. Phys. Chem.*, 1963, **67**, 1367; R. Srinivasan, *J. Am. Chem. Soc.*, 1964, **86**, 3318; R. Srinivasan and K. A. Hill, *ibid.*, 1965, **87**, 4988; R. Srinivasan and K. H. Carlough, *ibid.*, 1967, **89**, 4932.
3 R. S. H. Liu and G. S. Hammond, *J. Am. Chem. Soc.*, 1967, **89**, 4936.
4 J. C. Bünzli, A. J. Burak, and D. C. Frost, *Tetrahedron*, 1973, **29**, 3735.
5 R. Gleiter and W. Sander, *Angew. Chem.*, 1985, **97**, 575; *Angew. Chem., Int. Ed. Engl.*, 1985, **24**, 566.
6 W. L. Dilling, *Chem. Rev.*, 1966, **66**, 373.
7 R. Gleiter, W. Sander, H. Irngartinger, and A. Lenz, *Tetrahedron Lett.*, 1982, **23**, 2647.
8 Y. Inoue, S. Hagiwara, Y. Daino, and T. Hakushi, *J. Chem. Soc., Chem. Commun.*, 1985, 1307.
9 M. Ohsaku, *Tetrahedron Lett.*, 1986, **27**, 1797; M. Ohsaku, *J. Chem. Soc., Perkin Trans. 2*, 1987, 1027.
10 J. S. Binkley, M. J. Frisch, D. J. DeFrees, K. Raghavachari, R. A. Whiteside, H. B. Schlegel, E. M. Fluder, and J. A. Pople, Program Gaussian 82, 1982, Carnegie-Mellon University, Washington, DC.
11 H. B. Schlegel, *J. Comput. Chem.*, 1982, **3**, 214; P. Pulay, in 'Applications of Electronic Structure Theory,' ed. H. F. Schaefer III, Plenum, New York, NY, 1977.
12 J. S. Binkley, J. A. Pople, W. J. Hehre, *J. Am. Chem. Soc.*, 1980, **102**, 939; M. S. Gordon, J. S. Binkley, J. A. Pople, W. J. Pietro, and W. J. Hehre, *ibid.*, 1982, **104**, 2797.
13 W. J. Hehre, R. Ditchfield, and J. A. Pople, *J. Chem. Phys.*, 1972, **56**, 2257; A. Szabo and N. S. Ostlund, 'Modern Quantum Chemistry: Introduction to Advanced Electronic Structure Theory,' Macmillan, 1982.
14 (*a*) L. Møller and M. S. Plessett, *Phys. Rev.*, 1934, **46**, 618; (*b*) J. S. Binkley and J. S. Pople, *Int. J. Quantum Chem.*, 1975, **9**, 229.
15 J. A. Pople and R. K. Nesbet, *J. Chem. Phys.*, 1954, **22**, 571.
16 T. Amos and G. G. Hall, *Proc. R. Soc. London, Sect. A*, 1961, **263**, 483.
17 H. B. Schlegel, *J. Chem. Phys.*, 1986, **84**, 4530; *J. Phys. Chem.*, 1988, **92**, 3075.
18 P. J. Knowles and N. C. Handy, *J. Phys. Chem.*, 1988, **92**, 3097; *Chem. Phys. Lett.*, 1984, **111**, 315; *J. Chem. Phys.*, 1988, **88**, 6991.
19 K. Yamaguchi, Y. Takahara, T. Fueno, and K. N. Houk, *Theor. Chim. Acta*, 1988, **73**, 337.
20 P. N. Skancke, N. Koga, and K. Morokuma, *J. Am. Chem. Soc.*, 1989, **111**, 1559.
21 For example, D. S. Kemp, and F. Vellaccio, 'Organic Chemistry,' Worth, New York, NY, 1980.

Paper 9/02287B
Received 1*st June* 1989
Accepted 25*th September* 1989